Value of ^{18}F-3,4-Dihydroxyphenylalanine PET/MR Image Fusion in Pediatric Supratentorial Infiltrative Astrocytomas: A Prospective Pilot Study

Giovanni Morana[1], Arnoldo Piccardo[2], Claudia Milanaccio[3], Matteo Puntoni[4], Paolo Nozza[5], Armando Cama[6], Daniele Zefiro[7], Massimo Cabria[2], Andrea Rossi[1], and Maria Luisa Garrè[3]

[1]Unità Operativa di Neuroradiologia, Istituto G. Gaslini, Genoa, Italy; [2]Struttura Complessa di Medicina Nucleare, Ospedali Galliera, Genoa, Italy; [3]Unità Operativa di Neuro-oncologia, Istituto G. Gaslini, Genoa, Italy; [4]Direzione Scientifica, Ospedali Galliera, Genoa, Italy; [5]Unità Operativa di Anatomia Patologica, Istituto G. Gaslini, Genoa, Italy; [6]Unità Operativa di Neurochirurgia, Istituto G. Gaslini, Genoa, Italy; and [7]Struttura Complessa di Fisica Sanitaria, Ospedali Galliera, Genoa, Italy

Infiltrative astrocytomas (IAs) represent a group of astrocytic gliomas ranging from low-grade to highly malignant, characterized by diffuse invasion of the brain parenchyma. When compared with their adult counterpart, pediatric IAs may be considered biologically distinct entities; nevertheless, similarly to those in adults they represent a complex oncologic challenge. The aim of this study was to investigate the diagnostic role, clinical contribution, and prognostic value of fused ^{18}F-3,4-dihydroxyphenylalanine (^{18}F-DOPA) PET/MR images in pediatric supratentorial IAs. **Methods:** Pediatric patients with supratentorial IAs involving at least 2 cerebral lobes, either newly diagnosed or with suspected disease progression, prospectively underwent ^{18}F-DOPA PET and conventional MR imaging, performed within 10 d of each other. ^{18}F-DOPA PET data were interpreted qualitatively and semiquantitatively, fusing images with MR images. PET scans were classified as positive if tumors identified on MR imaging exhibited tracer uptake above the level of the corresponding contralateral normal brain. Maximum standardized uptake values, tumor–to–normal contralateral tissue ratios, and tumor–to–normal striatum ratios were calculated for all tumors. Correlations between the degree and extent of ^{18}F-DOPA uptake, MR imaging tumor characteristics, and histologic results were investigated. The contribution of ^{18}F-DOPA PET/MR image fusion was considered relevant if it enabled one to select the most appropriate biopsy site, discriminate between disease progression and treatment-related changes, or influence treatment strategy. The patient's outcome was finally correlated with ^{18}F-DOPA uptake. **Results:** Thirteen patients (8 boys and 5 girls) were included (5 diffuse astrocytomas, 2 anaplastic astrocytomas, 5 gliomatosis cerebri, and 1 glioblastoma multiforme). The ^{18}F-DOPA uptake pattern was heterogeneous in all positive scans (9/13), revealing metabolic heterogeneities within each tumor. Significant differences in terms of ^{18}F-DOPA uptake were found between low- and high-grade lesions ($P < 0.05$). The diagnostic and therapeutic contribution of ^{18}F-DOPA PET/MR image fusion was relevant in 9 of 13 patients (69%). ^{18}F-DOPA uptake correlated significantly with progression-free survival ($P = 0.004$). **Conclusion:** Our results indicate that ^{18}F-DOPA PET/MR image fusion may be a reliable imaging biomarker of pediatric IAs. Information gathered by this combined imaging approach can be readily transferred to the everyday practice and may help clinicians to better stratify patients with IAs, especially diffuse astrocytomas and gliomatosis cerebri, for diagnostic, therapeutic, and prognostic purposes.

Key Words: ^{18}F-DOPA PET; pediatric; brain tumor; MRI

Infiltrative astrocytomas (IAs) comprise a heterogeneous group of astrocytic gliomas ranging from low-grade to highly malignant, characterized by diffuse infiltration of tumor cells into the brain parenchyma (1). When compared with their adult counterparts, pediatric IAs show significantly different frequencies of genomic alterations and divergent mechanisms of tumorigenesis (2,3) and may be considered biologically distinct entities (4); nevertheless, similarly to those in adults, they represent a complex oncologic challenge (5). The known limitations of conventional MR imaging in IA characterization and follow-up (i.e., the limited ability to define tumor boundaries, to demonstrate tumor heterogeneity, and to differentiate between treatment-induced changes and residual or recurrent disease), in addition to the limited value of tissue biopsy as a representative sample of the entire tumor and the little consensus about the optimal treatment strategy, have critical diagnostic, therapeutic, and prognostic implications (5,6). In this scenario, novel imaging biomarkers, capable of providing noninvasive evaluation of the biologic activity of the whole lesion, may potentially help clinicians in the management of affected patients.

A growing body of evidence suggests that PET imaging of brain tumors with amino-acid analogs provides useful insights into tumor metabolism and may play a role in a more precise evaluation of brain tumors (7), especially when correlated with structural MR imaging data (8). When compared with ^{18}F-FDG, presently the most widely available PET tracer, amino-acid analogs have shown higher sensitivity to gliomas because of the higher tumor–to–normal-tissue background ratios (9). Among amino-acid PET tracers, ^{18}F-3,4-dihydroxyphenylalanine (^{18}F-DOPA) is largely unexplored in pediatric brain tumors, with only 3 children evaluated in prior studies (10,11), and no data are available specifically regarding IAs. In this prospective study, we evaluated the diagnostic role, clinical contribution, and prognostic value of fused ^{18}F-DOPA PET/MR images in a selected population of pediatric patients with supratentorial IAs.

MATERIALS AND METHODS

Subjects

The present study received Institutional Review Board approval. A written informed consent form was signed by all patients or their legal guardians, and patient assent was obtained when appropriate. Patients were prospectively recruited by the Neuro-oncology Unit of our Institution from 2009 to 2012. We included patients younger than 18 y with histologically proven supratentorial IAs involving at least 2 cerebral lobes, either newly diagnosed and with no previous treatment except biopsy or with suspected disease progression on MR imaging after chemo- and radiotherapy. Patients with small lesions, located in noneloquent areas and amenable of safe gross total surgical resection, were not included.

Image Protocol and Analysis

^{18}F-DOPA was purchased from a commercial supplier (IASOdopa; IASON Labormedizine Ges.Mbh & Co. KG). Data were obtained with a dedicated PET/CT system (Discovery ST; GE Healthcare) using the 3-dimensional mode with a scanning time of 30 min. The patients fasted for at least 4 h before ^{18}F-DOPA PET/CT. Brain scans were acquired 20 min after injection of 185 MBq of ^{18}F-DOPA in all patients. Carbidopa premedication was not used. A nondiagnostic low-dose CT scan (120 kV, 80 mA, 0.6 s per rotation) was used for attenuation correction.

MR imaging studies were performed on a 1.5-T magnet (Intera Achieva; Philips) and included 3-mm-thick axial fluid attenuation inversion recovery (FLAIR) and T2-weighted images, 4-mm-thick axial T1-weighted images, and 3-mm-thick coronal T2-weighted and FLAIR images. After gadolinium compound bolus administration (0.1 mmol/kg), 4-mm-thick axial, coronal, and sagittal T1-weighted images and a 3-dimensional T1-weighted turbo field echo sequence were acquired. ^{18}F-DOPA PET and MR imaging scans were obtained within 10 d of each other in all patients.

All ^{18}F-DOPA PET studies were interpreted qualitatively and semiquantitatively, fusing the images with MR images. Fusion was obtained automatically using a commercially available registration image software tool (Oncentra Masterplan TPS station, version 4.1; Nucletron). ^{18}F-DOPA PET images were fused to axial FLAIR, T2-weighted, and postcontrast T1-weighted images. PET scans were classified as positive if tumors identified on MR imaging exhibited tracer uptake above the level of the corresponding contralateral normal brain tissue.

A circular region of interest (ROI; diameter, 8 mm) was manually drawn over the tumor area displaying the highest ^{18}F-DOPA PET uptake. If increased ^{18}F-DOPA PET uptake was absent, the ROI was placed in the center of the MR imaging lesion. The radiotracer concentration in the ROI was normalized to the injected dose per patient's body weight, and the maximum standardized uptake value (SUVmax; g/mL) was obtained for each lesion. For the normal reference tissue, an ROI of the same size was mirrored to the matching contralateral normal brain. Another same-sized ROI was drawn over the contralateral normal striatum; in particular, this ROI was placed in the center of the putamen. Ratios of tumor to normal tissue uptake were generated by dividing the tumor SUVmax by the SUVmax of the contralateral normal brain region (T/N) and of the normal striatum (T/S).

Three main tumor uptake patterns were defined: absence of increased ^{18}F-DOPA uptake, characterized by a tumor uptake not exceeding the uptake of the matching contralateral normal brain region (T/N $\leq$ 1) and lower uptake than normal striatum (T/S < 1); moderately increased ^{18}F-DOPA uptake, characterized by a tumor uptake exceeding the uptake of the contralateral normal brain but remaining lower than or equal to that of the normal striatum (T/N > 1 and T/S $\leq$ 1); and markedly increased ^{18}F-DOPA uptake, in which tumor uptake clearly exceeded that observed in the contralateral normal brain region and striatum (T/N > 1 and T/S > 1).

On the basis of prior studies with radiolabeled amino acids (12,13), the absence of increased tumor tracer uptake suggested either an indolent tumor or a nontumoral lesion. Markedly increased ^{18}F-DOPA uptake was suggestive of a highly active tumor, and moderately increased ^{18}F-DOPA uptake was interpreted as an intermediate condition (i.e., mild to moderately biologically active tumor).

Diagnostic and Clinical Contribution Analysis

Conventional MR imaging tumor characteristics and extent were correlated with ^{18}F-DOPA uptake. Given the diffuse nature of the disease, MR imaging tumor extent was delineated on the basis of T2/FLAIR signal abnormalities (14). The correlation between the degree of ^{18}F-DOPA uptake, histologic results, and World Health Organization (WHO) tumor grade was also determined.

The contribution of ^{18}F-DOPA PET/MR image fusion was considered relevant if it enabled one to select the most appropriate biopsy site, to discriminate between disease progression and treatment-related changes, or to influence treatment strategy, thereby supplementing the role of MR imaging and histology.

Disease Monitoring and Outcome

Follow-up MR imaging studies were performed every 3–6 mo to monitor the disease status and treatment outcome. Conventional MR imaging evaluation was based on changes in tumor size on FLAIR and T2-weighted images (14). Tumor volume was assessed using the diameter method, as previously described (15). We defined partial response as a greater than 50% reduction in tumor volume, compared with baseline measurements; progressive disease (PD) as a greater than 25% increase in tumor volume; and stable disease as any other status not meeting the criteria for complete response, partial response, or PD (14).

Statistical Analysis

Descriptive statistics included mean, SD, median, first and third quartile, and minimum and maximum of continuous factors; in the case of categoric factors, number and percentage distribution were used. Box plots were used to graphically describe the distribution of continuous variables, and a Mann–Whitney U test was used to analyze the statistical difference between categories. Kaplan–Meier estimates of the cumulative probability of progression-free survival (PFS), defined as the interval between initial diagnosis, onset of PD, and mortality from any cause, were obtained. All analyses were conducted using SPSS software (version 15.0; SPSS Inc.). Two-tailed probabilities were reported, and a P value of 0.05 was used to define nominal statistical significance.

RESULTS

Subjects

The main characteristics of patients, tumors, and ^{18}F-DOPA PET/MR imaging are summarized in Supplemental Table 1 (supplemental materials are available at http://jnm.snmjournals.org).

Thirteen patients (8 boys and 5 girls; age range, 6–17 y; mean age, 11 y) were eligible for this study. ^{18}F-DOPA PET/MR imaging fusion was performed before biopsy in 5 patients and after biopsy in 6. In the remaining 2, ^{18}F-DOPA PET/MR imaging fusion was performed because of suspected disease progression after treatment with chemotherapy (temozolomide) and radiotherapy. In all, there were 11 patients with newly diagnosed untreated lesions and 2 previously treated patients with suspected disease progression. Because 1 patient (case 10) underwent an additional ^{18}F-DOPA PET/MR imaging fusion follow-up scan, fourteen ^{18}F-DOPA PET/MR imaging fusion studies were performed in this 13-patient cohort. Histologic results were as follows: 5 diffuse astrocytomas (DAs) (WHO grade II); 2 anaplastic astrocytomas (AAs) (WHO grade III); 1 glioblastoma multiforme (GBM) (WHO grade IV); and 5 gliomatosis cerebri (GC), with biopsy samples showing 2 DAs (WHO grade II), 2 AAs (WHO grade III), and 1 GBM (WHO grade IV).

Diagnostic and Clinical Contribution

On MR imaging, all lesions showed increased T2/FLAIR signal intensity and variable (iso- to hypointense) appearance on T1-weighted imaging. After administration of contrast material, no areas of pathologic enhancement were demonstrated, with the exception of 1 patient (case 13) with GC (GBM histology). Regarding ^{18}F-DOPA PET/MR imaging fusion, 9 of 13 tumors showed increased tracer uptake (positive scans) (Supplemental Table 1). The uptake pattern was inhomogeneous in all positive scans, revealing metabolic heterogeneities within each tumor. In positive scans of newly diagnosed untreated lesions, increased ^{18}F-DOPA uptake was concordant with T2/FLAIR tumor extent in 5 patients, smaller in 1, and larger in 1.

All AAs and GBMs showed areas of markedly increased tracer uptake, whereas all DAs showed absent to moderately increased tracer uptake. Of the 5 patients with GC, 1 with a DA histology showed moderately increased uptake, whereas 4 showed markedly increased uptake (1 with DA, 2 with AA, and 1 with GBM on histology) (Fig. 1). SUVmax, T/N, and T/S ratios of all lesions are reported in Supplemental Table 1. A significant difference regarding ^{18}F-DOPA uptake was found between low- and high-grade tumors ($P < 0.05$) (Fig. 2).

The contribution of ^{18}F-DOPA PET/MR imaging fusion was relevant in 9 of 13 patients and double in 1 patient (case 10) (Supplemental Table 1). In patients scanned before biopsy, ^{18}F-DOPA PET/MR imaging fusion was helpful for selecting the most appropriate biopsy site in the 2 positive scans. In these 2 patients (cases 7 and 11), ^{18}F-DOPA PET/MR imaging fusion showed heterogeneous uptake (moderately to markedly increased) within diffuse nonenhancing MR imaging lesions. Biopsy from areas of markedly increased uptake guided by ^{18}F-DOPA PET/MR imaging fusion revealed AA.

Regarding the differentiation between disease progression and treatment-related changes, 2 patients with nonenhancing high-grade tumors (cases 6 and 12) showed an interval increase in the extension of T2/FLAIR abnormalities after temozolomide and radiotherapy, suspected for nonenhancing disease progression. In one of them (case 12), ^{18}F-DOPA PET/MR imaging fusion showed the absence of tracer uptake, suggesting absence of active disease; the known tumor components presented markedly increased tracer uptake. Follow-up MR imaging at 8 mo showed stable T2/FLAIR abnormalities, suggesting radiation-induced changes. However, in this patient, unequivocal nonenhancing disease progression was demonstrated infratentorially, outside the radiotherapy field, 5 mo after the end of treatment. In the other patient (case 6) (Fig. 3), ^{18}F-DOPA PET/MR imaging fusion showed moderately to markedly increased tracer uptake in nonenhancing areas, consistent with tumor progression.

^{18}F-DOPA PET/MR imaging fusion influenced treatment strategy, supplementing the role of conventional MR imaging and histology, in 5 patients. In 4 of them, harboring low-grade DA (cases 1, 2, 4, and 5), absent ^{18}F-DOPA uptake (Fig. 4) warranted conservative management (wait and see), avoiding further tumor debulking and medical therapy.

In a patient (case 10) with GC and DA histology (WHO grade II), ^{18}F-DOPA uptake was extensively and markedly increased, suggesting a more aggressive behavior (Figs. 1A and 1B); clinical conditions were also deteriorating. An aggressive treatment with chemo- (temozolomide) and radiotherapy implemented, supported by ^{18}F-DOPA PET data. In this patient, follow-up MR imaging performed 4 mo after the end of radiotherapy revealed enlarged T2/FLAIR abnormalities; clinical conditions were also worse. As we felt unable to reliably differentiate radiation-induced edema from sudden nonenhancing disease progression, we elected to obtain another ^{18}F-DOPA PET scan. ^{18}F-DOPA PET/MR imaging fusion showed the absence of increased uptake within the new T2/FLAIR abnormalities, suggesting radiation-induced edema. Subsequent follow-up MR imaging demonstrated marked reduction of signal abnormalities, confirming the ^{18}F-DOPA PET/MR imaging fusion results. However, even in this patient unequivocal nonenhancing disease progression was demonstrated 8 mo later in the contralateral cerebral hemisphere. Of note, in another patient (case 9) with the same diagnosis of GC and DA histology, ^{18}F-DOPA PET/MR imaging fusion revealed heterogeneous areas of moderately increased tracer uptake. This patient received only a first-line treatment with chemotherapy (temozolomide), as intended before a PET scan based on histology and clinical conditions.

The treatment strategy was not influenced by ^{18}F-DOPA PET/MR imaging results in patients with high-grade tumors.
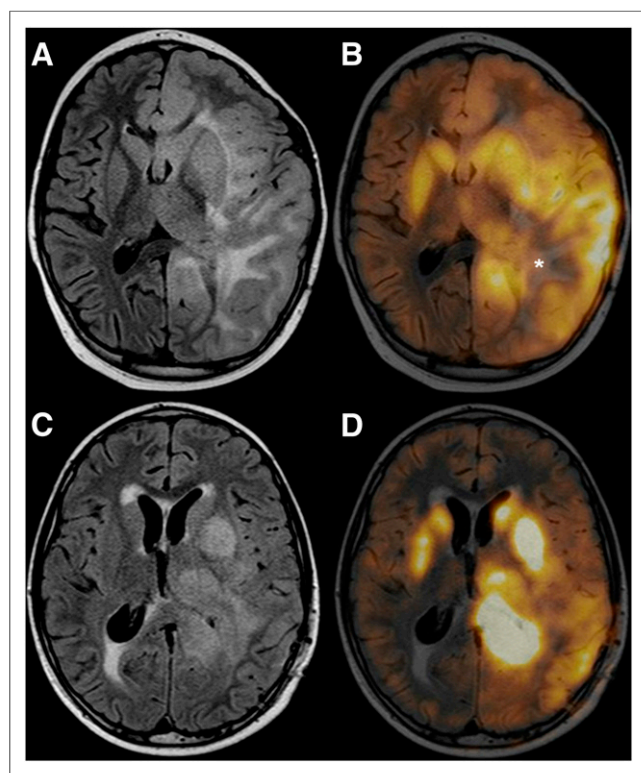

FIGURE 1. (A and B) GC (WHO grade II) (case 10). Extensive left hemispheric lesion with ipsilateral involvement of basal ganglia and thalamus (FLAIR image, A). ^{18}F-DOPA PET/MR imaging fusion (B) shows areas of moderately to markedly increased tracer uptake (T/N, 2.3; T/S, 1.2) concordant with tumor extent. Notice absence of tracer uptake within areas suggestive of vasogenic edema (*, B). Biopsy sample performed before PET presumably undergraded lesion. (C and D) GC (WHO grade IV) (case 13). ^{18}F-DOPA PET MR imaging fusion (D) shows areas of moderately to markedly increased tracer uptake (T/N, 2.3; T/S, 1.4) in left hemisphere extending beyond FLAIR tumor extent (C).

Outcome

PFS and overall survival (OS) of all patients are shown in Figure 5. All 4 patients (cases 1, 2, 4, and 5) without increased tracer uptake, followed with a wait-and-see approach, had stable disease (median follow-up, 29 mo; range, 8–44 mo). Similarly, 2 patients (cases 3 and 9) with a moderately increased tracer uptake, treated with chemotherapy, had partial response and stable disease
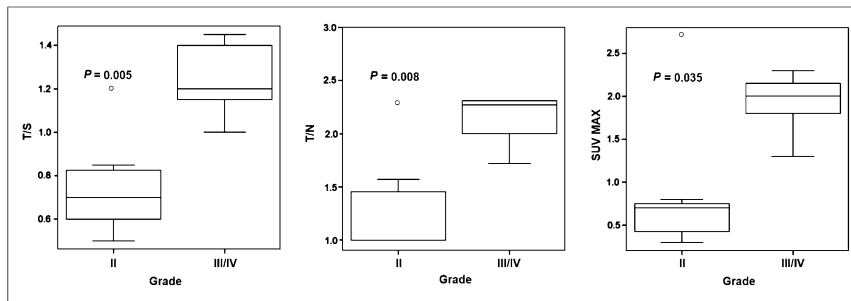
FIGURE 2. Box plots representing ^{18}F-DOPA T/S, T/N, and SUVmax for WHO grades II and III–IV lesions. Significant difference regarding ^{18}F-DOPA uptake is demonstrated between low- and high-grade tumors. Outlier (°) is case 10.

on follow-up (median follow-up, 26 mo; range, 20–32 mo), respectively. On the contrary, of the 7 patients showing markedly increased tracer uptake, 6 (cases 6, 7, 10, 11, 12, and 13) developed PD (median follow-up, 8.5 mo; range, 4–25 mo), whereas 1 (case 8) demonstrated stable disease (follow-up, 20 mo). We found statistically significant differences ($P = 0.004$) regarding PFS (Fig. 5) between patients with absent to moderately increased uptake (T/S $\leq$ 1) versus those with markedly increased uptake (T/S $>$ 1, corresponding to T/N $>$ 1.6).

DISCUSSION

IAs are complex diagnostic and therapeutic challenges in children. From a diagnostic standpoint, conventional postcontrast MR imaging does not always allow for a precise delineation of tumor margins and has limited sensitivity and specificity in defining tumor grade. Because the blood–brain barrier is frequently preserved, evaluation of tumor extent basically relies on T2-weighted and FLAIR images. However, the latter do not reliably discriminate among infiltrative disease, peritumoral edema, and treatment-related changes. Furthermore, little information can be drawn regarding intralesional histologic heterogeneity, biologic activity, or aggressiveness of the disease. Thus, the contribution of conventional MR imaging toward therapeutic decision making remains unsatisfactory (6). Tissue biopsy is the gold standard to define the histologic type and grade but also suffers from certain limitations in

IAs; in fact, it provides only information about the sampled portion of the neoplasm, leading to inaccurate results when biopsy samples are not taken from the most malignant region (16). From a clinical perspective, optimal treatment is still unclear, because total surgical resection may be impossible or ethically unacceptable given the extent and the diffuse nature of the disease; different therapeutic approaches based on chemotherapy, radiotherapy, or a combination of both are usually contemplated depending on the histologic grade, patient's age, and clinical conditions. Wait and see may be an option for WHO grade II lesions.

Given the extreme variability in the clinical course and outcome of IAs, novel imaging modalities are currently under evaluation for a better diagnostic and prognostic stratification; these include both advanced MR imaging techniques (i.e., diffusion-weighted imaging, perfusion imaging, and MR spectroscopy) and amino-acid analog PET tracers (7,17–19). Molecular PET imaging with amino-acid analogs is emerging as a valuable modality, not competing with but rather complementing MR imaging. Among radiolabeled amino-acids, ^{18}F-DOPA PET imaging provides more accurate visualization of high-grade, low-grade, and recurrent tumors than ^{18}F-FDG PET in adults, demonstrating results similar to ^{11}C-methionine (MET), at present the best-studied radiolabeled amino acid. The major drawback of ^{11}C-MET, however, is the short half-life (~20 min), which limits its widespread use (20,21). ^{18}F-fluoroethyl-L-tyrosine (^{18}F-FET) is the second most widely studied amino-acid tracer for brain tumors in adults, with diagnostic performance comparable to that of ^{11}C-MET (7,22). Even though ^{18}F-FET and ^{18}F-DOPA have not been directly compared, indirect evaluation through comparison with ^{11}C-MET and ^{18}F-FDG reveals many similarities. Both tracers have relatively long half-lives (~110 min), allowing for widespread use without the need for an onsite cyclotron. The main difference between these 2 tracers is represented by the specific ^{18}F-DOPA uptake in the putamen and caudate nucleus. Unlike with ^{18}F-FET, this might potentially affect the ability to distinguish normal brain from adjacent tumor. On the other hand, the ^{18}F-DOPA uptake within the striatum gives the opportunity to further stratify tumoral uptake ratios through comparison with both the normal background levels and the striatum. In children, ^{18}F-DOPA has the advantage of being a multipurpose tracer that can be used in several conditions, including tumors producing an excess of catecholamine (such as neuroblastomas) (23) and in congenital hyperinsulinism (24), which might potentially have an impact on health care cost optimization.

A limited number of PET studies have been conducted in children harboring infiltrative tumors. Prior research demonstrates that ^{18}F-FDG and ^{11}C-MET improve the quality of therapeutic management of pediatric brain tumors at the diagnostic, surgical, and postoperative level, particularly in ill-defined infiltrative
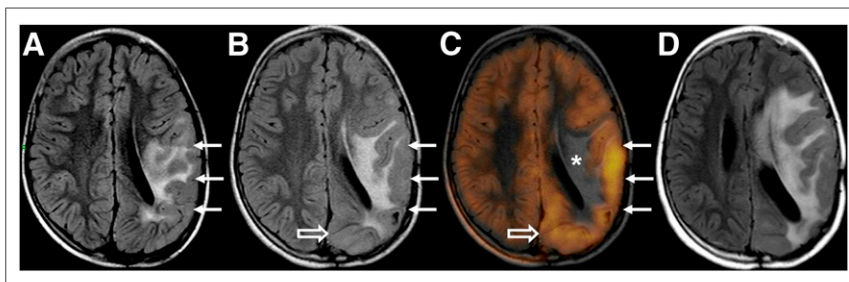

FIGURE 3. Anaplastic astrocytoma (WHO grade III). Differentiation between PD and treatment-related changes (case 6). Diffusely infiltrating lesion involving left frontoparietal region (thin arrows, A). MR imaging follow-up performed 3 mo after end of treatment (radiotherapy and temozolomide) revealed increased extension of FLAIR abnormalities, possibly representing edema or nonenhancing disease progression (open and thin arrows, B). There was no contrast enhancement on postcontrast MR imaging (not shown). ^{18}F-DOPA PET/MR imaging fusion (C) shows areas of moderately to markedly increased tracer uptake, in keeping with active disease. Notice absence of tracer uptake within areas of supposed vasogenic edema (*, C). Subsequent MR imaging (D) performed 2 mo later confirmed PD.
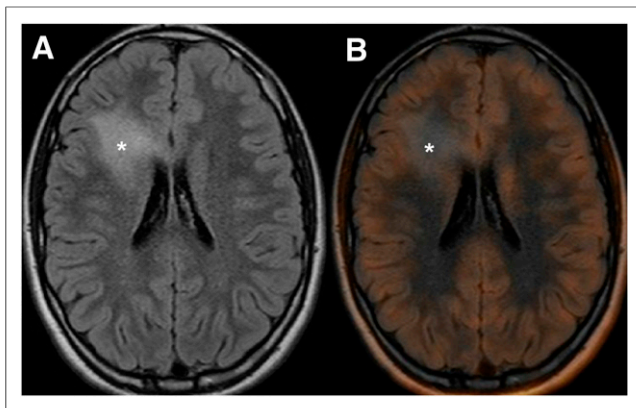
FIGURE 4. (A and B) Diffuse astrocytoma (WHO grade II) (case 4). Diffusely infiltrating lesion (*, FLAIR image, A) demonstrating absence of tracer uptake on ^{18}F-DOPA PET/MR imaging fusion (*, B).

tumors. ^{18}F-FDG presents some limitations in defining targets for biopsy in low-grade pediatric tumors, whereas ^{11}C-MET appears also to be a better tracer than ^{18}F-FDG for delineating tumor boundaries and for residual tumor detection (25,26). Other studies found a correlation between ^{18}F-FDG uptake and tumor malignancy; however, there was significant overlap between different grades of malignancy (27,28). A recent study evaluated the association of MR imaging and ^{18}F-FDG PET in pediatric diffuse intrinsic brain stem gliomas, demonstrating that if ^{18}F-FDG uptake involves at least half the tumor, survival is poor (29). More recently, a method of registering ^{18}F-FDG PET with MR permeability images was developed in children with brain tumors, mainly infiltrative gliomas (30). Regarding ^{18}F-FET, the utility of this tracer to plan stereotactic biopsy in 2 children with diffusely infiltrating tumors has been reported (31). Few reports have described the role of PET in GC. Increased ^{11}C-MET uptake and decreased ^{18}F-FDG uptake have been reported in children, suggesting the valuable role of ^{11}C-MET PET to identify neoplastic tissue (32).

To the best of our knowledge, there have been no published studies regarding the role of ^{18}F-DOPA PET in pediatric patients with IAs. In our study, the degree of tumoral ^{18}F-DOPA uptake accurately reflected the biologic nature of pediatric IAs; in fact, we were able to demonstrate significant differences in the uptake ratios between patients harboring low-grade and high-grade IAs. Furthermore, ^{18}F-DOPA PET demonstrated in vivo metabolic heterogeneity of IAs, providing noninvasive information about the bi-

ologic activity of the whole lesion, thus helping in guiding biopsy. It is tempting to speculate that, had ^{18}F-DOPA PET/MR imaging fusion been performed before biopsy in all patients, its contribution to biopsy guidance might have been much higher. In untreated PET-positive tumors, the extent of increased ^{18}F-DOPA PET uptake was also helpful to improve our confidence in defining tumor boundaries.

We also demonstrated the usefulness of ^{18}F-DOPA PET in posttreatment surveillance, particularly in discriminating between nonenhancing disease progression and treatment-related changes. Increased tracer uptake was found in nonenhancing disease progression, whereas absence of tracer uptake was suggestive of radiation-induced changes. Because an objective MR imaging criterion for nonenhancing tumor progression is currently regarded unfeasible (33), ^{18}F-DOPA PET deserves consideration given its promising role in this challenging field.

The contribution of ^{18}F-DOPA PET/MR imaging fusion was also relevant in the therapeutic decision-making process so as to plan an individualized treatment strategy in patients with low-grade DA and GC. In particular, we adopted a wait-and-see approach in all patients with DA and absence of increased tracer uptake; as demonstrated in other studies with amino-acid analog tracers (12,13), this patient subgroup may be considered at a lower risk of subsequent tumor progression, thus justifying a conservative approach when a complete surgical removal may not safely be achieved.

In GC patients, ^{18}F-DOPA PET/MR imaging fusion also proved complementary to MR imaging and histology; to the best of our knowledge, this is the largest pediatric series of GC studied with an amino-acid analog PET tracer. Stratification of GC according to histologic grade is difficult and undergrading is a well-known limitation of GC biopsy because of the diffusely infiltrating nature of the lesion (34). Integration of ^{18}F-DOPA PET/MR imaging data with histologic results allowed a more precise characterization of the whole lesion, providing additional diagnostic information for patient care. In particular, in the 2 patients with GC and identical histology of WHO grade II DA obtained before ^{18}F-DOPA PET/MR imaging fusion studies, we found 2 different uptake patterns: moderately and markedly increased, respectively. Despite similar histologic data and tumor extent, clinical conditions and biologic behavior of the lesion were worse in the patient with markedly increased tracer uptake, highlighting the fact that histology presumably underestimated the real nature of the tumor, likely because of sampling from a lower grade area.

In patients with high-grade tumors, treatment strategy was not influenced by ^{18}F-DOPA PET/MR imaging because surgery was mainly performed only to obtain tissue for histologic diagnosis, given the extent of the tumors, and medical treatment always consisted of combined chemotherapy and radiotherapy. A multimodality treatment combining surgery, local radiotherapy, and chemotherapy is the standard approach for children older than 3 y newly diagnosed with supratentorial high-grade astrocytomas (5), and there are not as many options as in low-grade diffuse infiltrating lesions (i.e., conservative management, or a variable combination of surgery, chemotherapy, or radiotherapy).

Finally, uptake ratios were highly correlated with prognosis. We found a significant prognostic difference between IAs with
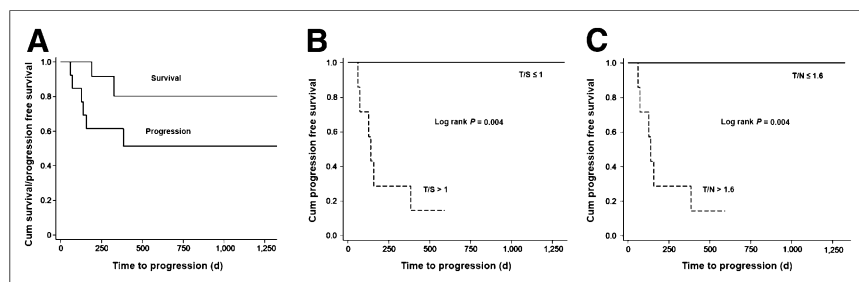

FIGURE 5. (A) Kaplan–Meier OS curves and PFS curves. (B and C) Kaplan–Meier plots of PFS according to T/S (B) and T/N (C). Statistically significant differences ($P = 0.004$) are demonstrated between patients with absent to moderately increased tracer uptake (T/S ≤ 1) versus those with markedly increased uptake (T/S > 1, corresponding to T/N > 1.6). Cum = cumulative.

absent to moderately increased tracer uptake and those with markedly increased uptake.

Among limitations of our study, we are aware of the relatively small sample of patients; however, our cohort included only patients with purely astrocytic diffusely infiltrating gliomas involving at least 2 cerebral lobes, which do not represent a common entity in children particularly for a single center. In addition, the population was heterogeneous concerning the timing of the PET scans in newly diagnosed lesions, with some studies performed before biopsy and others after; in patients studied with PET after biopsy, the histologic sampling might not have necessarily corresponded to the higher grade areas. Furthermore, evaluation of tumor size on the basis of T2 and FLAIR signal abnormality, according to the standard Response Assessment in Neuro Oncology criteria (*14,33*), might be biased by inadvertent inclusion of areas of nontumoral edema. Finally, median follow-up was also limited but nevertheless sufficient to discriminate between aggressive and nonaggressive tumors.

CONCLUSION

Our preliminary data suggest that ^{18}F-DOPA PET/MR imaging fusion in children with IAs correlates reliably with WHO tumor grade and outcome, is useful for biopsy planning and posttreatment monitoring, and contributes to stratification of patients with DA and GC, thereby influencing their management. Correlation with MR imaging is crucial for a comprehensive interpretation of PET results; therefore, close collaboration between nuclear medicine physicians and neuroradiologists is required to provide clinicians with more robust data. Information gathered by this combined approach can be readily transferred to the everyday practice and may be beneficial to tailor treatment strategies. Further experience on larger cohorts is required to better define the diagnostic and prognostic yield of this technique.

DISCLOSURE

REFERENCES

1. Fuller CE. Infiltrative astrocytomas (diffuse astrocytoma, anaplastic astrocytoma, glioblastoma). In: Adesina AM, ed. *Atlas of Pediatric Brain Tumors*. Berlin, Germany: Springer; 2010:25–38.
2. Jones DT, Mulholland SA, Pearson DM, et al. Adult grade II diffuse astrocytomas are genetically distinct from and more aggressive than their paediatric counterparts. *Acta Neuropathol.* 2011;121:753–761.
3. Paugh BS, Qu C, Jones C, et al. Integrated molecular genetic profiling of pediatric high-grade gliomas reveals key differences with the adult disease. *J Clin Oncol.* 2010;28:3061–3068.
4. Nishikawa R. Pediatric and adult gliomas: how different are they? *Neuro-oncol.* 2010;12:1203–1204.
5. Broniscer A, Gajjar A. Supratentorial high-grade astrocytoma and diffuse brainstem glioma: two challenges for the pediatric oncologist. *Oncologist.* 2004;9:197–206.
6. Vossough A, Nabavizadeh SA. Functional imaging based diagnostic strategy: intraaxial brain masses. In: Scott HF, Feroze BM, eds. *Functional Neuroradiology, Principles and Clinical Application*. New York, NY: Springer; 2011:197–220.
7. Heiss WD, Raab P, Lanfermann H. Multimodality assessment of brain tumors and tumor recurrence. *J Nucl Med.* 2011;52:1585–1600.
8. Ledezma CJ, Chen W, Sai V, et al. ^{18}F-FDOPA PET/MRI fusion in patients with primary/recurrent gliomas: initial experience. *Eur J Radiol.* 2009;71:242–248.
9. Chen W, Silverman DH. Advances in evaluation of primary brain tumors. *Semin Nucl Med.* 2008;38:240–250.
10. Tripathi M, Sharma R, D'Souza M, et al. Comparative evaluation of F-18 FDOPA, F-18 FDG, and F-18 FLT-PET/CT for metabolic imaging of low grade gliomas. *Clin Nucl Med.* 2009;34:878–883.
11. Morana G, Piccardo A, Garrè ML, Nozza P, Consales A, Rossi A. Multimodal magnetic resonance imaging and ^{18}F-L-dihydroxyphenylalanine positron emission tomography in early characterization of pseudoresponse and nonenhancing tumor progression in a pediatric patient with malignant transformation of ganglioglioma treated with bevacizumab. *J Clin Oncol.* 2013;31:e1–e5.
12. Pirotte BJ, Lubansu A, Massager N, et al. Clinical interest of integrating positron emission tomography imaging in the workup of 55 children with incidentally diagnosed brain lesions. *J Neurosurg Pediatr.* 2010;5:479–485.
13. Floeth FW, Pauleit D, Sabel M, et al. Prognostic value of O-(2-^{18}F-fluoroethyl)-L-tyrosine PET and MRI in low-grade glioma. *J Nucl Med.* 2007;48:519–527.
14. van den Bent MJ, Wefel JS, Schiff D, et al. Response assessment in neurooncology (a report of the RANO group): assessment of outcome in trials of diffuse low-grade gliomas. *Lancet Oncol.* 2011;12:583–593.
15. Sorensen AG, Patel S, Harmath C, et al. Comparison of diameter and perimeter methods for tumor volume calculation. *J Clin Oncol.* 2001;19:551–557.
16. Kleihues P, Cavenee WK. *Pathology and Genetics of Tumors of the Nervous System.* Lyon, France: IARC Press; 2000:10–21.
17. Cha S. Update on brain tumor imaging: from anatomy to physiology. *AJNR.* 2006;27:475–487.
18. Chang SM, Nelson S, Vandenberg S, et al. Integration of preoperative anatomic and metabolic physiologic imaging of newly diagnosed glioma. *J Neurooncol.* 2009;92:401–415.
19. Herholz K, Langen KJ, Schiepers C, Mountz JM. Brain tumors. *Semin Nucl Med.* 2012;42:356–370.
20. Becherer A, Karanikas G, Szabó M, et al. Brain tumour imaging with PET: a comparison between [^{18}F]fluorodopa and [^{11}C]methionine. *Eur J Nucl Med Mol Imaging.* 2003;30:1561–1567.
21. Chen W, Silverman DH, Delaloye S, et al. ^{18}F-FDOPA PET imaging of brain tumors: comparison study with ^{18}F-FDG PET and evaluation of diagnostic accuracy. *J Nucl Med.* 2006;47:904–911.
22. Grosu AL, Astner ST, Riedel E, et al. An interindividual comparison of O-(2-[^{18}F]fluoroethyl)-L-tyrosine (FET)- and L-[methyl-^{11}C]methionine (MET)-PET in patients with brain gliomas and metastases. *Int J Radiat Oncol Biol Phys.* 2011;81:1049–1058.
23. Piccardo A, Lopci E, Conte M, et al. Comparison of ^{18}F-dopa PET/CT and ^{123}I-MIBG scintigraphy in stage 3 and 4 neuroblastoma: a pilot study. *Eur J Nucl Med Mol Imaging.* 2012;39:57–71.
24. Ribeiro MJ, De Lonlay P, Delzescaux T, et al. Characterization of hyperinsulinism in infancy assessed with PET and ^{18}F-fluoro-L-DOPA. *J Nucl Med.* 2005;46:560–566.
25. Pirotte B, Goldman S, Salzberg S, et al. Combined positron emission tomography and magnetic resonance imaging for the planning of stereotactic brain biopsies in children: experience in 9 cases. *Pediatr Neurosurg.* 2003;38:146–155.
26. Pirotte BJ, Lubansu A, Massager N, et al. Clinical impact of integrating positron emission tomography during surgery in 85 children with brain tumors. *J Neurosurg Pediatr.* 2010;5:486–499.
27. Borgwardt L, Hojgaard L, Carstensen H, et al. Increased fluorine-18 2-fluoro-2-deoxy-D-glucose (FDG) uptake in childhood CNS tumors is correlated with malignancy grade: a study with FDG positron emission tomography/magnetic resonance imaging coregistration and image fusion. *J Clin Oncol.* 2005;23:3030–3037.
28. Utriainen M, Metsahonkala L, Salmi TT, et al. Metabolic characterization of childhood brain tumors: comparison of ^{18}F-fluorodeoxyglucose and ^{11}C-methionine positron emission tomography. *Cancer.* 2002;95:1376–1386.
29. Zukotynski KA, Fahey FH, Kocak M, et al. Diffuse intrinsic brain stem glioma: a report from the pediatric brain tumor consortium. *J Nucl Med.* 2011;52:188–195.
30. Zukotynski KA, Fahey FH, Vajapeyam S, et al. Exploratory evaluation of MR permeability with ^{18}F-FDG PET mapping in pediatric brain tumors: a report from the Pediatric Brain Tumor Consortium. *J Nucl Med.* 2013;54:1237–1243.
31. Messing-Jünger AM, Floeth FW, Pauleit D, et al. Multimodal target point assessment for stereotactic biopsy in children with diffuse bithalamic astrocytomas. *Childs Nerv Syst.* 2002;18:445–449.
32. Cai L, Gao S, Li Y, Lu D. ^{11}C-methionine or ^{11}C-choline PET is superior to MRI in the evaluation of gliomatosis cerebri. *Clin Nucl Med.* 2011;36:127–129.
33. Wen PY, Macdonald DR, Reardon DA, et al. Updated response assessment criteria for high-grade gliomas: response assessment in neuro-oncology working group. *J Clin Oncol.* 2010;28:1963–1972.
34. Fuller GN, Kros JM. Gliomatosis cerebri. In: Louis DN, Ohgaki H, Wiestler OD, Cavanee WK, eds. *WHO Classification of Tumours of the Central Nervous System.* Lyon, France: International Agency for Research on Cancer: 2007:50–52.